

Supplemental Information

Enhanced Optomechanical Properties of Mechanochemiluminescent Poly(methyl acrylate) Composites with Granulated Fluorescent Conjugated Microporous Polymer Fillers

*Yuan Yuan,^a Weiben Chen,^a Zhe Ma,^b Yakui Deng,^a Ying Chen,^a Yulan Chen^{*a}, and Wenping Hu^{*a}*

- a. Tianjin Key Laboratory of Molecular Optoelectronic Science, Department of Chemistry, Tianjin University, Tianjin 300354, P. R. China.
Collaborative Innovation Centre of Chemical Science and Engineering, Tianjin 300072, P. R. China.
E-mail: yulan.chen@tju.edu.cn; huwp@tju.edu.cn.
- b. School of Materials Science and Engineering, Tianjin University, Tianjin 300354, P. R. China.

Table of Contents

1. Experimental Procedures	
Materials and methods	3
Experimental Details	3-5
2. Results and Discussion	
FT-IR spectra of CMPs and granulated CMPs (Figure S3)	5
Solid-state ¹³ C CP/MAS NMR spectra of granulated CMPs (Figure S4)	5
TGA curves of granulated CMPs (Figure S5)	6
Powder X-ray diffraction profiles of granulated CMPs (Figure S6)	6
Nitrogen adsorption/desorption isotherms of CMPs and granulated CMPs (Figure S7)	6
Microscopic images of CMPs and granulated CMPs (Figure S8)	7
SEM images of CMPs and granulated CMPs (Figure S9)	7
TEM images of CMPs and granulated CMPs (Figure S10)	8
AFM images of TPE-CMP and granulated TPE-CMP (Figure S11)	8
AFM images of TPA-CMP and granulated TPA-CMP (Figure S12)	9
The maximum emission and fluorescence quantum efficiency of CMPs and granulated CMPs (Table S2)	9
FT-IR spectra of CMP/PMA composites (Figure S13)	9
TGA curves of CMP/PMA composites (Figure S14)	10
DSC curves (second heating process) of CMP/PMA composites (Figure S15)	10
SEM images of fracture surface of CMP/PMA composites (Figure S16)	11
Optical images of CMP composite films (Figure S17)	11
Setup for the optomechanical tests (Figure S18)	12
Stress and light intensity vs strain during stretching of TPA-0.28% (Figure S19)	12
3. Supplementary Videos	12
4. References	13

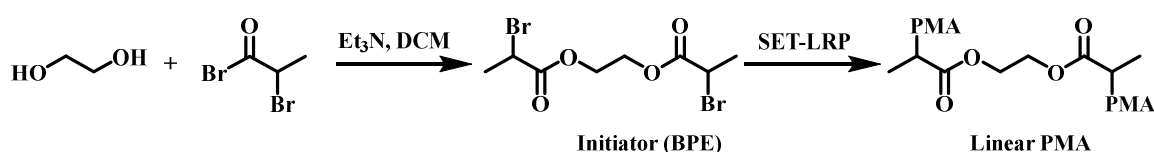
Experimental Procedures

Materials and Methods

General: Cu (0) wire was purchased from Sigma-Aldrich. Tris[2-(dimethylamino)ethyl]amine (Me6-TREN) and 2-bromopropionyl bromide were purchased from J&K Scientific. 2,2'-Azobis(2-methylpropionitrile) (AIBN) was purchased from Energy Chemical and recrystallized in methanol before used. Ethylene glycol, methyl acrylate (MA) and triethylamine (TEA) were purchased from Tianjin Jiangtian Chemical Company. MA purified by passing through a short column of neutral Al₂O₃ prior to use in order to remove the radical inhibitor. TEA was distilled under argon over CaH₂ prior to use. 5,5'/7'-Bisacrylate-5,5'/7'-dihydroxyethylenoxyadamantylideneadamantane 1,2-dioxetane was prepared according to literature procedures.^[1] Solvents were purified according to standard procedures.

Measurements. The CMPs were ball-milled with a planetary ball mill (QM-3SP04) purchased from the Nanjing University Instrument Limited. Sonication dispersed experiments were carried out with a Sonics VCX 500 Watt Ultrasonic processor purchased from Sonics and Materials Inc, and a 13 mm probe was used at a frequency of 20 kHz, at 30% of the maximum amplitude. The ¹H NMR spectra were recorded on a Bruker AVANCE III-400 NMR spectrometer under 25 °C by using CDCl₃ as the solvent. Gel Permeation Chromatography (GPC) of the sample was carried out using a Shimadzu LC-20AD, GPC system. FT-IR spectra were collected in reflection mode on a Bruker Alpha spectrometer with a scan range of 400-4000 cm⁻¹. The UV-Vis absorption and diffuse reflectance spectra were obtained on a PerkinElmer Lambda 750 spectrophotometer with standard procedure. Fluorescence spectra were recorded on a Hitachi F-7000 fluorescence spectrophotometer. The nitrogen adsorption and desorption isotherms were measured at 77 K using a Bel Japan Inc. model BELSOPR-mini II analyser and the samples were degassed at 100 °C for 3 h under vacuum (10⁻⁵ bar) before analysis. Powder X-ray diffraction experiment was carried out on Rigaku SmartLab X-ray diffractometer. The images of CMPs and granulated CMPs were performed on a Nikon microscope (ECLIPSE LV100ND). Field emission scanning electron microscopies (FE-SEM) were performed on a Hitachi Limited model SU800 microscope. The CMP/PMA composite films were fractured at room temperature and SEM images were taken after sputter-coating with platinum. TEM observations were performed using a Philips Tecnai G2F20 microscope at 200 kV. Thermal properties of polymers were evaluated using a thermogravimetric analysis (TGA) with a differential thermal analysis instrument (TA Instruments Q-50) over the temperature range from room temperature to 800 °C under nitrogen atmosphere with a heating rate of 10 °C min⁻¹. Differential scanning calorimetry (DSC) measurements were conducted using the TA Instruments Q-20 with a scan rate of 5 °C/min.

Experimental Details



Scheme S1. Synthetic routes of linear PMA.

Synthesis of the initiator bis(2-bromopropionyl) ethane (BPE): Triethylamine (5.8 mL, 0.04 mol) and ethylene glycol (1.24 g, 0.02 mol) were dissolved in 100 mL of dry dichloromethane. Then, the solution was cooled with an ice bath. 2-Bromopropionyl bromide (9.8 mL, 0.08 mol) was added dropwise. The reaction was allowed to warm to room temperature and stirred overnight. The suspension obtained was filtered, and the filtrate was washed with 1M HCl, followed by 5% aqueous solution of NaHCO₃ and water. The organic layers were combined and dried over MgSO₄, filtered, and then concentrated. The crude product was purified by flash column chromatography and provided colorless oil (2.78 g, 42% yield). ¹H NMR (400 MHz, CDCl₃) δ: 4.42-4.39 (m, 6H), 1.83 (d, 6H).

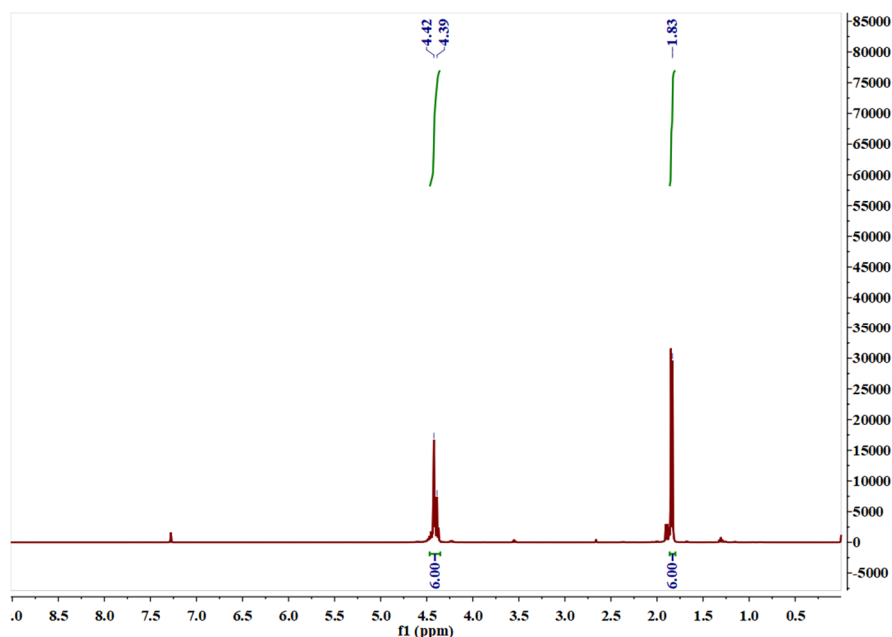


Figure S1. ^1H NMR spectrum of the initiator bis(2-bromopropionyl) ethane (BPE).

Synthesis of linear PMA: The single-electron transfer living radical polymerization (SET-LRP) process was carried out as literature.^[2] A solution of MA (5 mL, 0.061 mmol), DMSO (6 mL), Me6-TREN (53 mg, 0.230 mmol), and bis(2-bromopropionyl) ethane (BPE) (22 mg, 0.066 mmol) was prepared in a Schlenk flask. Then the removal of oxygen was accomplished by applying at least three freeze–pump–thaw cycles. After that, 5 cm of Cu (0) wire wrapped around a Teflon-coated stirring bar was loaded under positive argon pressure. Then placing the flask in a water bath thermostated at 25 °C with stirring. When the solution became viscously, THF was added into the solution to stop the reaction. The polymerization mixture was dissolved in 15 mL THF, passed through a small neutral Al_2O_3 chromatographic column to remove unreacted Cu(0) catalyst and Cu(II) compounds, and the resulting solution was concentrated and precipitated twice in cold methanol with stirring. Methanol was removed by decantation and the final colorless polymer was dried under vacuum. The M_n and M_w/M_n values were determined by GPC with DMF solvent and PMMA standards, $M_n=78\text{K}$, $M_w/M_n=1.28$.

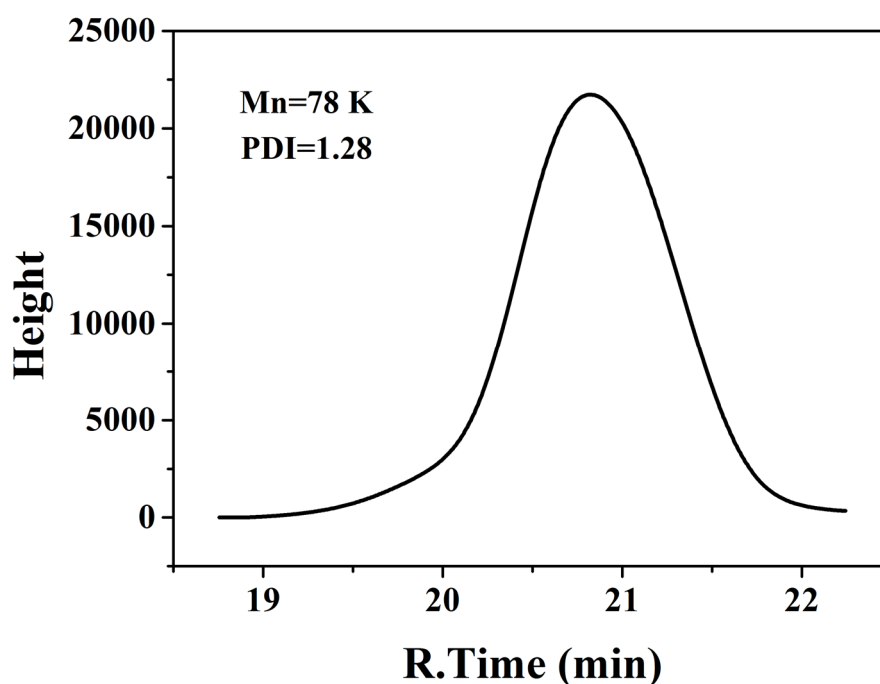


Figure S2. GPC trace of linear PMA.

Table S1. Feed ratios of blank PMA film and CMP/PMA composite films.

	Linear PMA (mg)	Granulated CMPs suspensions (mL)	THF (mL)	MP (mg)	AIBN (mg)	MA (mL)	Weight fraction of CMPs
Blank	200	0	1.5	10	20	2.0	0
TPE-0.28%	200	0.5	1.0	10	20	2.0	0.28%
TPE-0.54%	200	1.0	0.5	10	20	2.0	0.54%
TPE-0.79%	200	1.5	0	10	20	2.0	0.79%
TPA-0.28%	200	0.5	1.0	10	20	2.0	0.28%
TPA-0.80%	200	1.0	0.5	10	20	2.0	0.80%
TPA-0.83%	200	1.5	0	10	20	2.0	0.83%

Results and Discussion

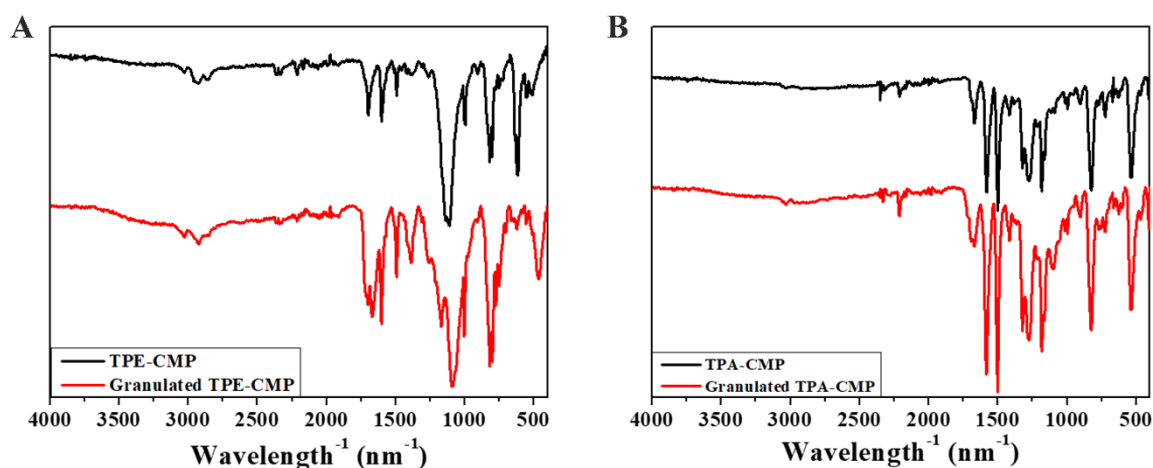


Figure S3. FT-IR spectra of (A) TPE-CMP and granulated TPE-CMP (B) TPA-CMP and granulated TPA-CMP.

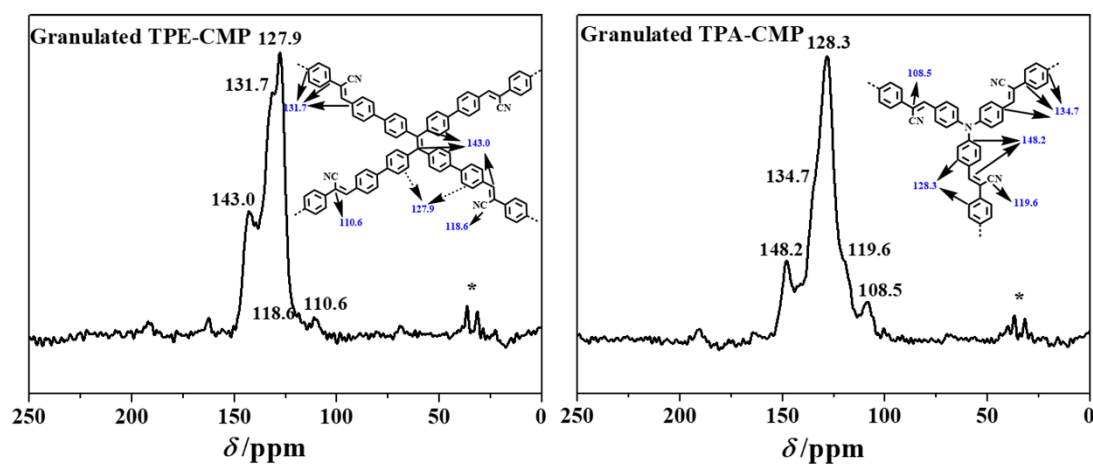


Figure S4. Solid-state ^{13}C CP/MAS NMR spectra of granulated TPE-CMP and granulated TPA-CMP. Asterisks denote spinning side bands.

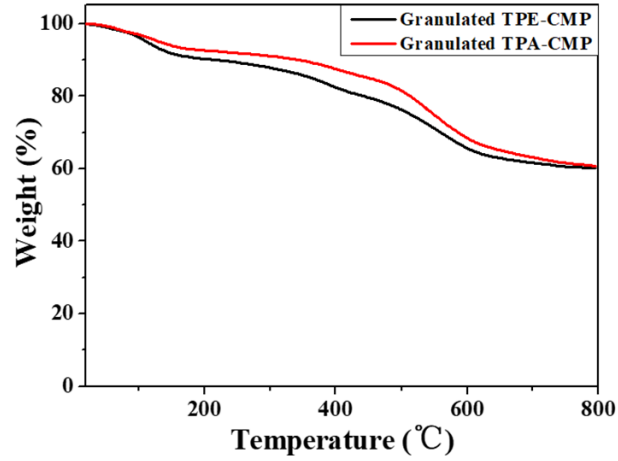


Figure S5. TGA curves of granulated CMPs.

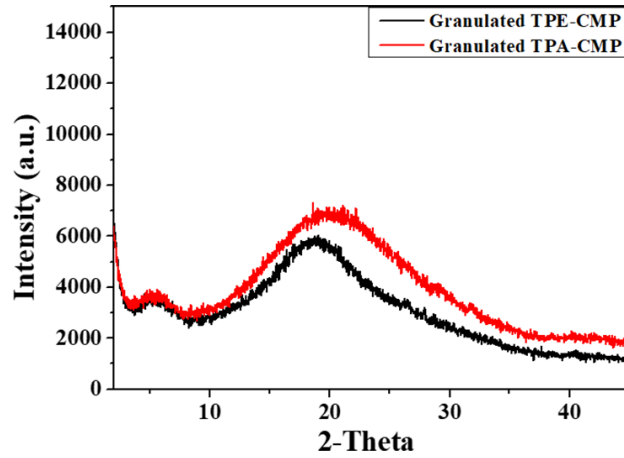


Figure S6. Powder X-ray diffraction profiles of granulated CMPs.

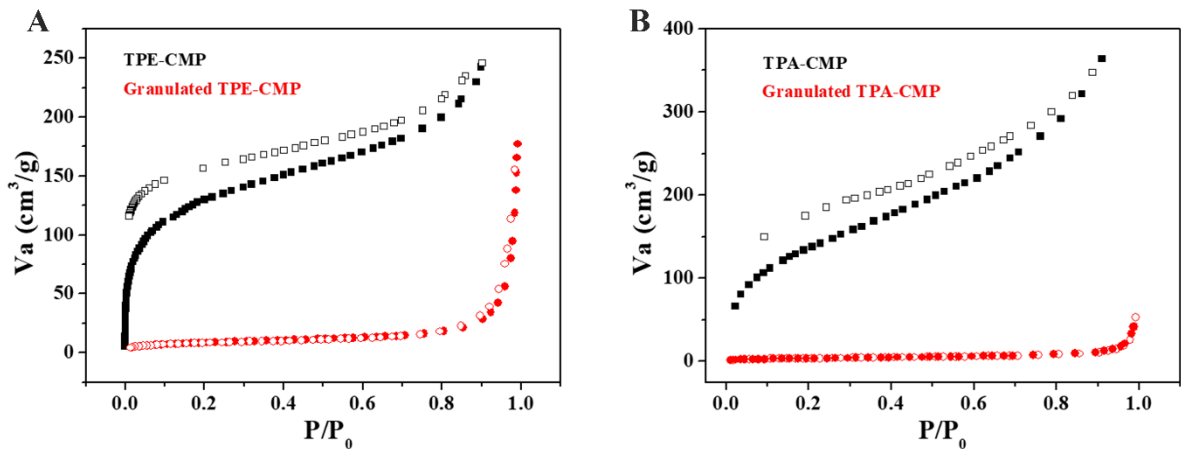


Figure S7. Nitrogen adsorption/desorption isotherms at 77K of (A) TPE-CMP and granulated TPE-CMP (B) TPA-CMP and granulated TPA-CMP.

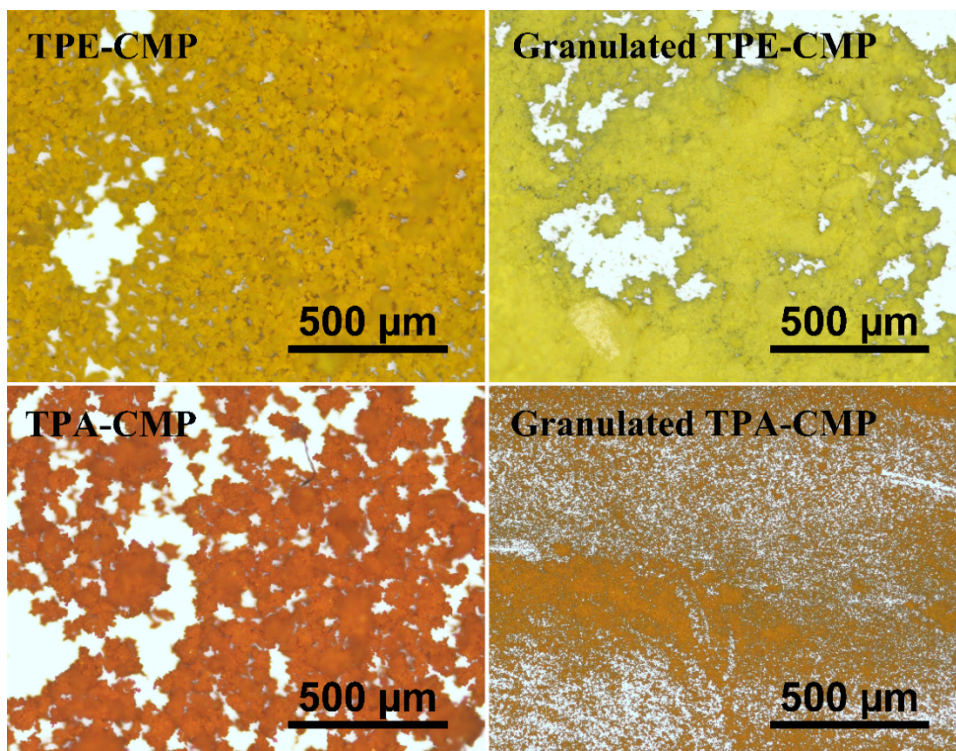


Figure S8. Microscopic images of CMPs and granulated CMPs.

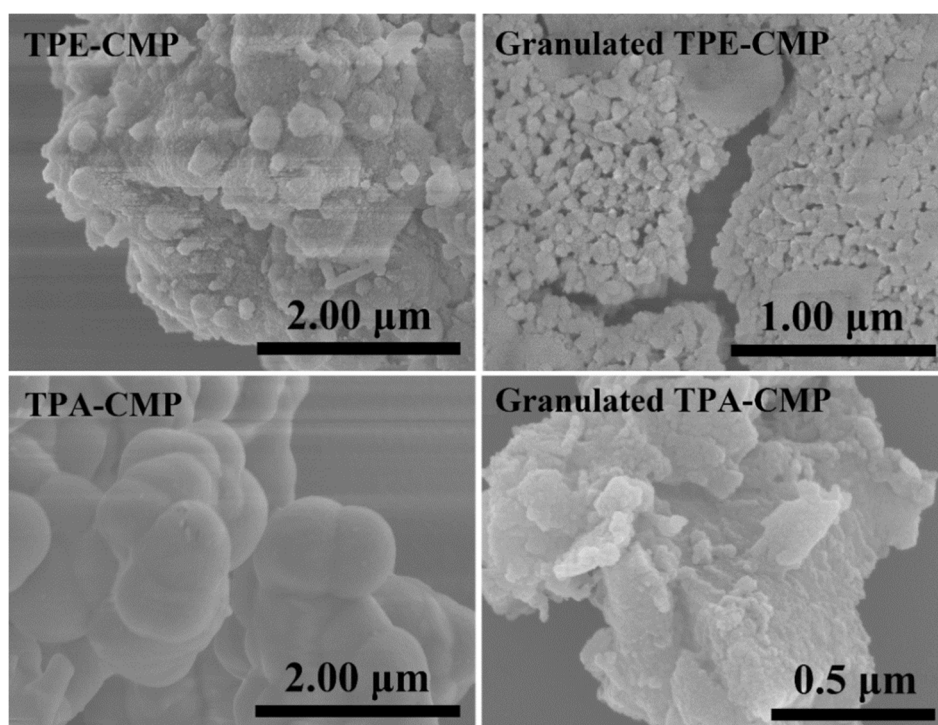


Figure S9. SEM images of CMPs and granulated CMPs.

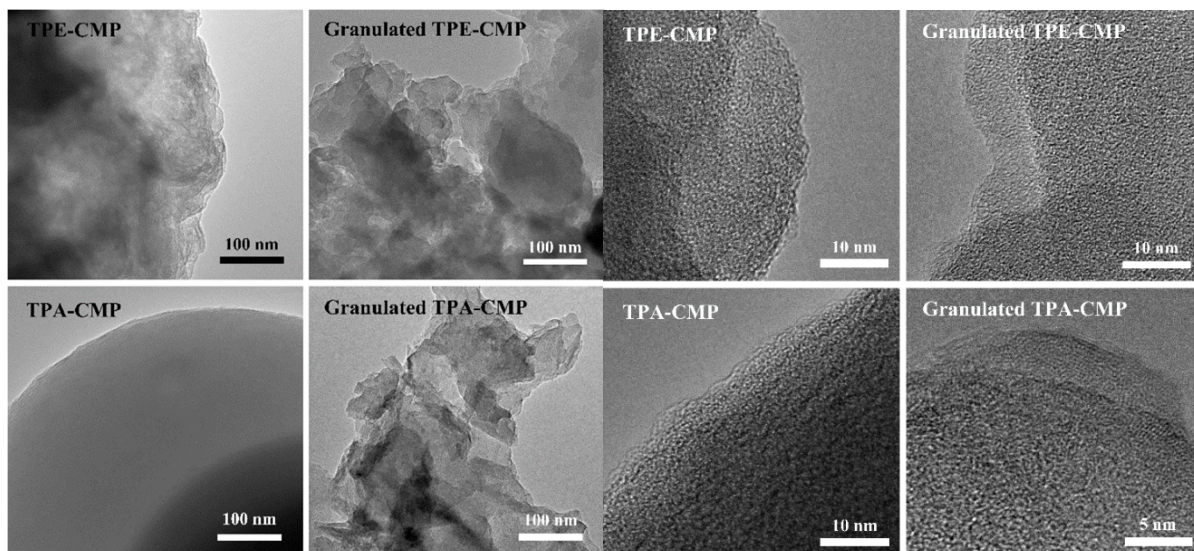


Figure S10. TEM images of CMPs and granulated CMPs.

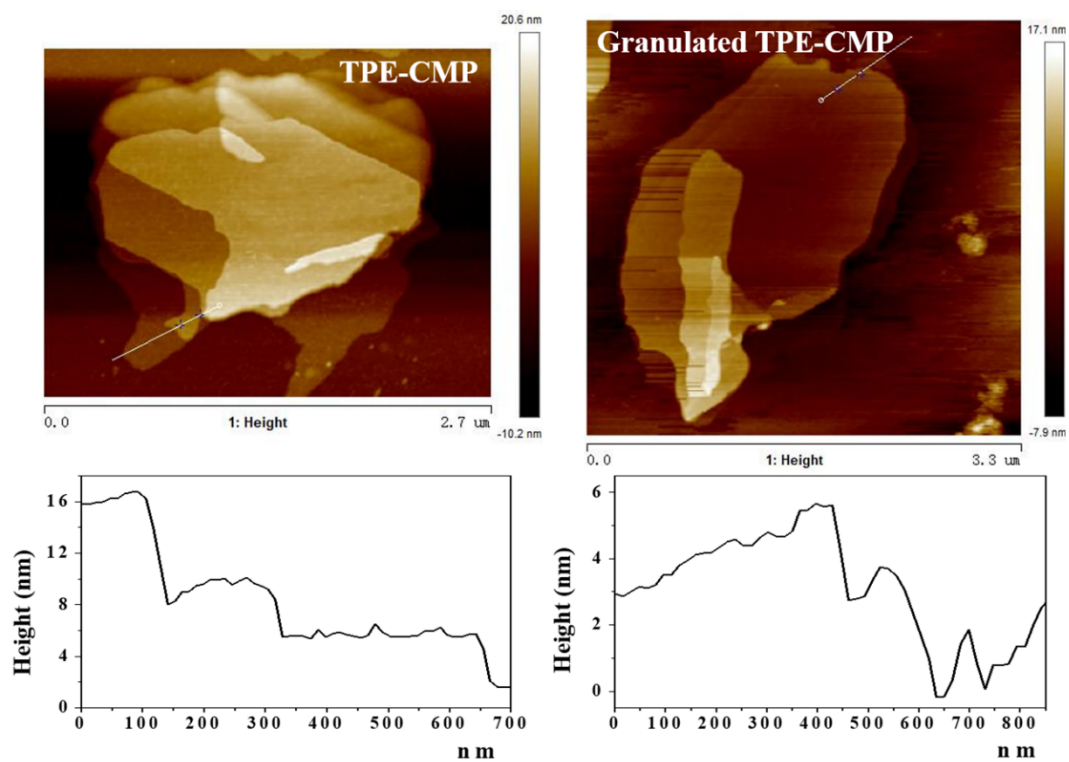


Figure S11. AFM images of TPE-CMP and granulated TPE-CMP and the corresponding height graphic analysis.

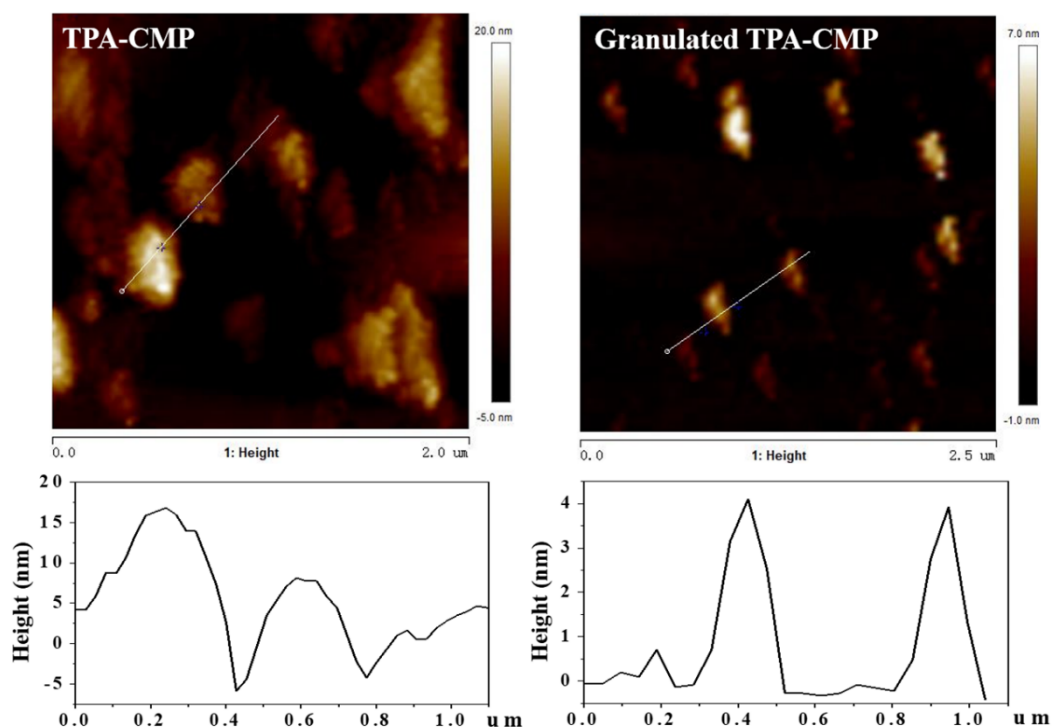


Figure S12. AFM images of TPA-CMP and granulated TPA-CMP and the corresponding height graphic analysis.

Table S2. The maximum emission and QY(%)^[a] of CMPs and granulated CMPs.

	TPE-CMP	Granulated TPE-CMP	TPA-CMP	Granulated TPA-CMP
Maximum emission	592 nm	549 nm	608 nm	603 nm
QY (%) ^[a]	16.6%	22.9%	4.4%	3.9%

^[a]fluorescence quantum efficiency (420 nm excited)

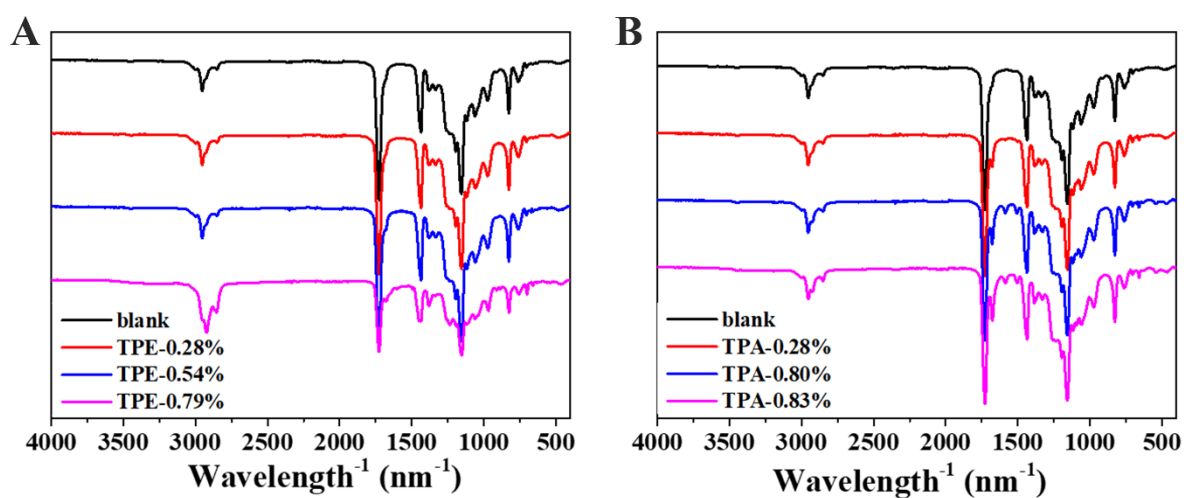


Figure S13. FT-IR spectra of (A) TPE-CMP/PMA films and (B) TPA-CMP/PMA films.

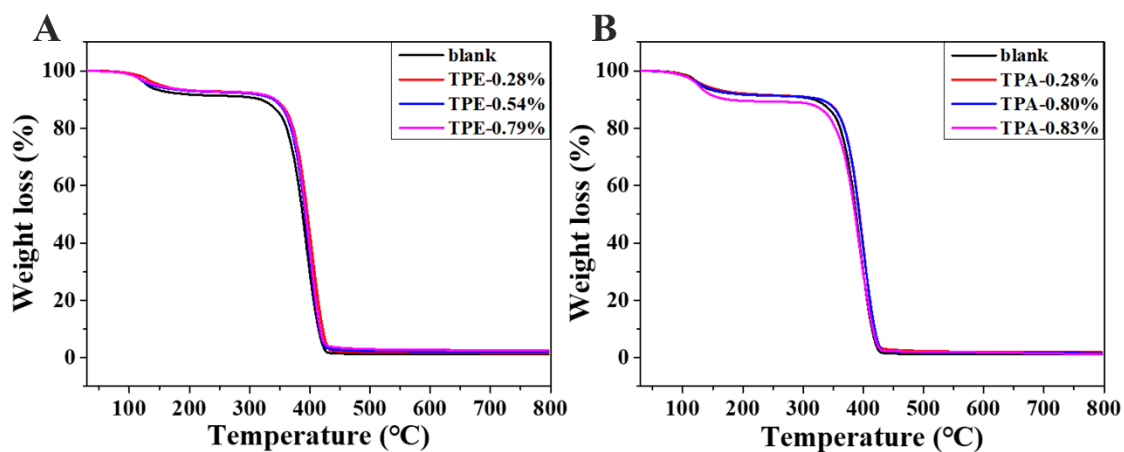


Figure S14. TGA curves of (A) TPE-CMP/PMA films and (B) TPA-CMP/PMA films.

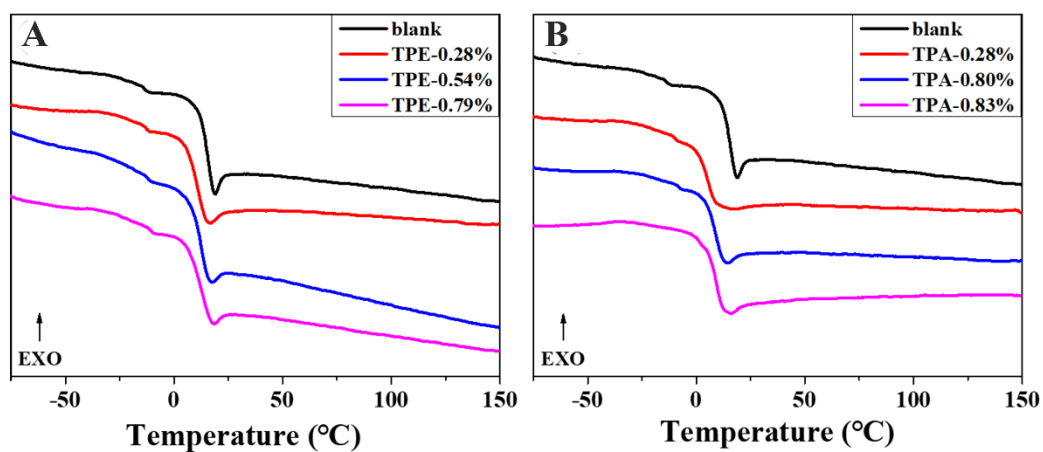


Figure S15. DSC curves (second heating process) of (A) TPE-CMP/PMA films and (B) TPE-CMP/PMA films.

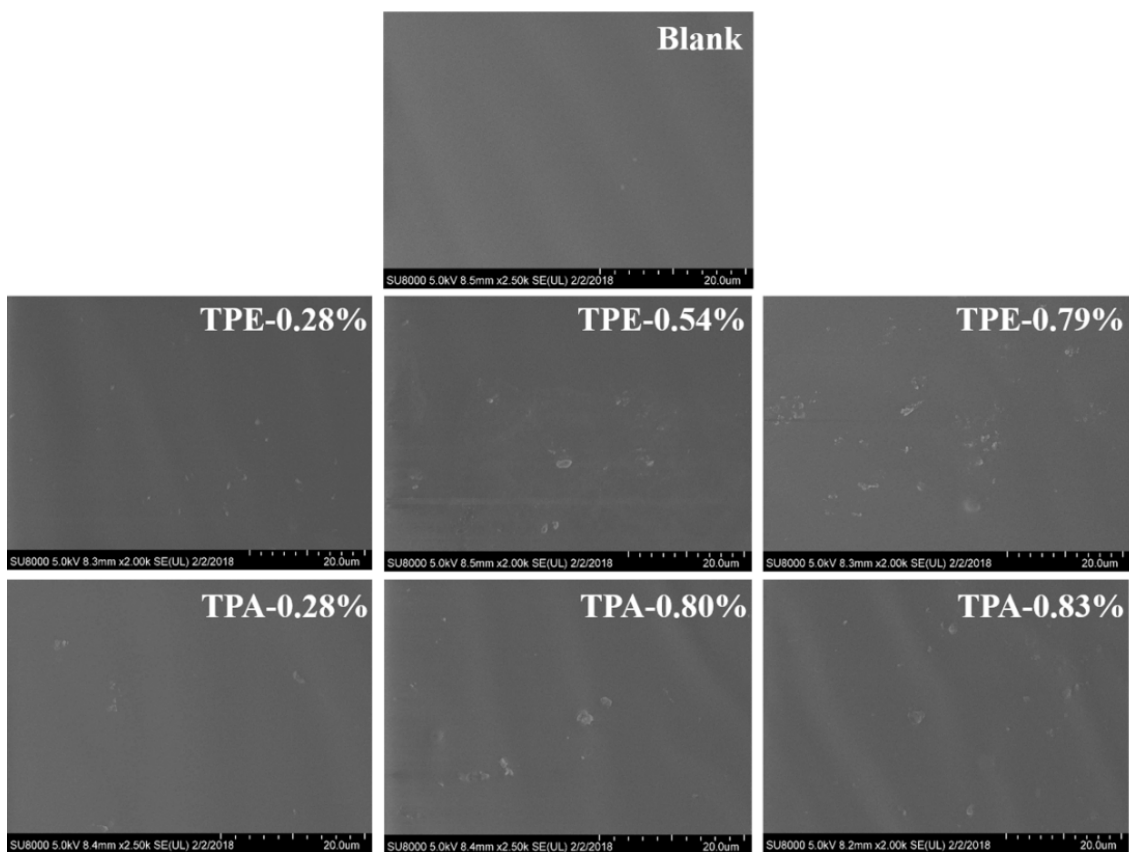


Figure S16. SEM images of fracture surface of blank film and CMPs composite films (scale bars are 20 μm).

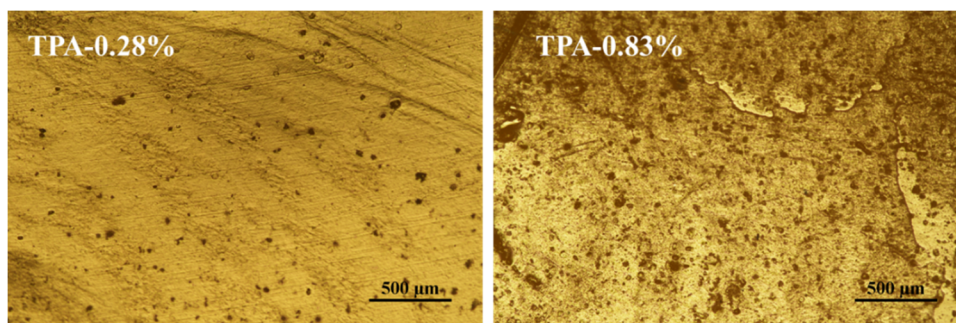


Figure S17. Optical images of CMP composite films.

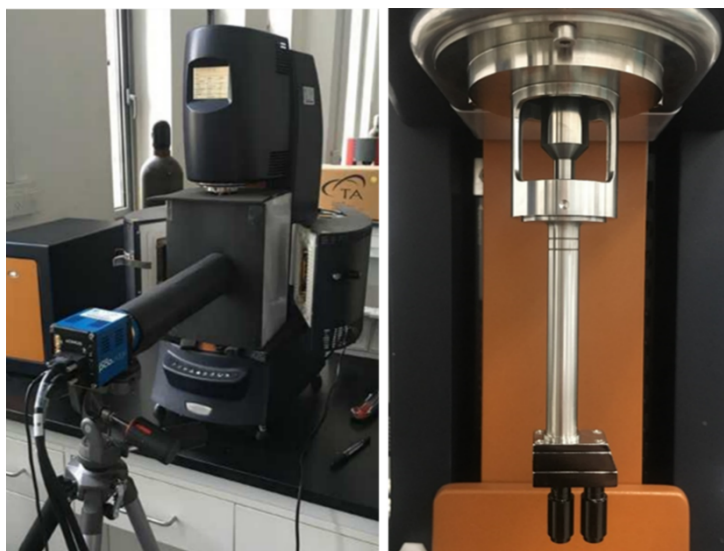


Figure S18. Setup for the optomechanical tests.

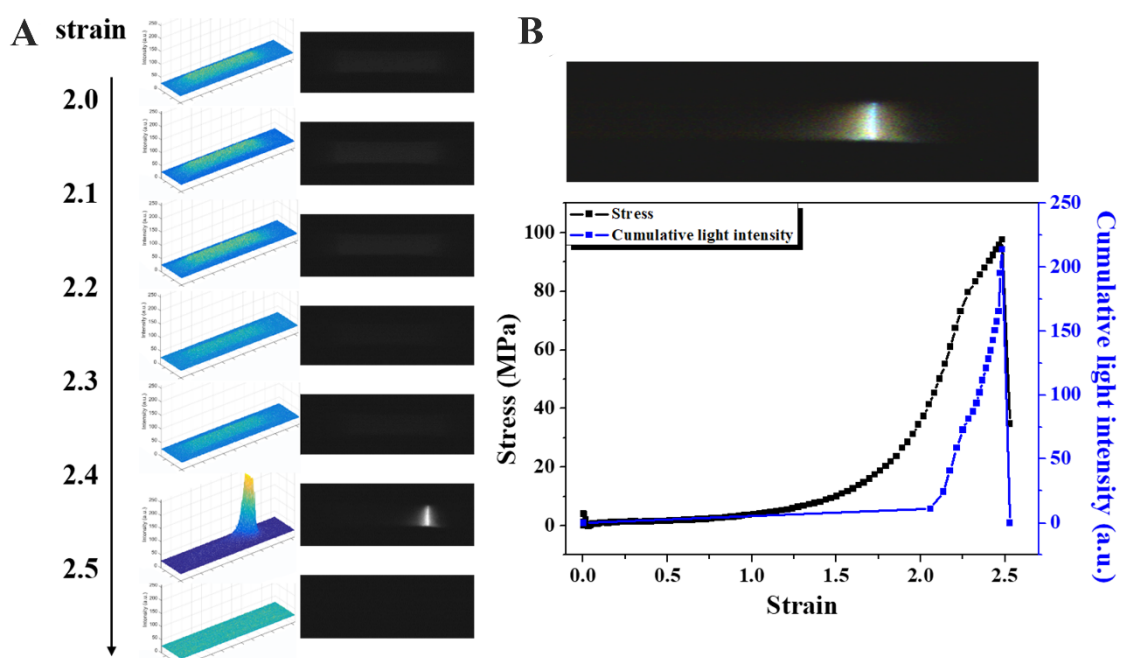


Figure S19. Stress and light intensity vs strain during stretching of **TPA-0.28%**: (A) monochromatic optical images and intensity analysis of the **TPA-0.28%** sample during stretching and (B) diagram of stress and light intensity vs strain (above is original pictures of **TPA-0.28%** at fracture).

Supplemental Videos

Video S1. Representative video of green chemiluminescence upon stretching a **TPE-CMP/PMA** composite film of **TPE-0.28%** crosslinked with 1,2-dioxetane (Video_S1).

Video S2. Representative video of white chemiluminescence upon stretching a **TPA-CMP/PMA** composite film of **TPA-0.28%** crosslinked with 1,2-dioxetane (Video_S2).

Video S3. Representative video of blue chemiluminescence upon stretching a bulk film of blank PMA crosslinked with 1,2-dioxetane (Video_S3).

All the videos were recorded at 200 fps and their display speed is kept at 8 fps.

References

[1] Y. Chen, A. J. Spiering, S. Karthikeyan, G. W. Peters, E. W. Meijer and R. P. Sijbesma, *Nat. Chem.*, 2012, **4**, 559-562.

[2] C. Zhang, J. Ling, Q. Wang, *Macromolecules*, 2011, **44**, 8739-8743.